Structure Effect on Water Diffusion and Hygroscopic Stress in Polyimide Films

JWO-HUEI JOU,* RITA HUANG, PEIR-TEH HUANG, and WEN-PING SHEN

Department of Materials Science and Engineering, Tsing Hua University, Hsin Chu 30043, Taiwan, Republic of China

SYNOPSIS

A bending-beam technique has been used to in situ monitor the diffusion of water in various polyimide films. The polyimides studied are pyromellitic dianhydride-4,4'-oxydianiline (PMDA-ODA), pyromellitic dianhydride-*p*-phenylenediamine (PMDA-PDA), and 3,3',4,4'-benzophenone tetracarboxylic dianhydride-*p*-phenylenediamine (BPDA-PDA), and their blends and random copolymers. The diffusion of water in these films obeys Fick's law. In PMDA-ODA, the mean diffusion constant is $5.2 \pm 0.4 \times 10^{-9}$ (cm^2/s) for thicknesses ranging from 6.7 to 27.3 μm. In PMDA-PDA, it is $2.0 \pm 0.4 \times 10^{-9}$ (cm^2/s) for thicknesses ranging from 7.3 to 20.0 μm, and in BPDA-PDA, $0.27 \pm 0.02 \times 10^{-9}$ (cm^2/s) for thicknesses ranging from 4.8 to 21.0 μm. In the blends and random copolymer with 50 wt % PMDA-ODA and 50 wt % PMDA-PDA, the diffusion constants are slightly smaller than those in the pure PMDA-ODA, but much larger than in the pure PMDA-PDA. On the contrary, in those with 50 wt % BPDA-PDA and 50 wt % PMDA-PDA, the diffusion constants are much smaller than those in the pure PMDA-PDA, but slightly larger than in the pure BPDA-PDA. These diffusion constants are primarily affected by the chemical structure of the imide molecule. The morphology, such as crystallinity, of the films has played a secondary factor. Hygroscopic stresses due to water uptake in all the studied films increase as the film thickness increases. It can be attributed to that the film orientation decreases with the increase of thickness.

INTRODUCTION

Polyimides have many important applications in microelectronic packaging.[1-5] They have various excellent properties, one of which is low dielectric constant. However, they have some shortcomings. They are, for example, high internal stress due to thermal mismatchment and poor adhesion with silicon or copper. These two drawbacks must be overcome in order to have sound mechanical performance. As to retaining or improving the dielectric property, uptake of water in the imide films should be minimized. Upon uptake of water, the dielectric constants and conductivities in polyimide films as well as the level of dielectric loss will increase.[6-8] If there exist trace amounts of ionic impurities in the imide films, the absorbed water may cause solvation and result in a significant increase in the film conductivity. If the solvated ions move to electrodes, they may further cause electrolytic corrosion. Besides, the dimension of imide films will be affected by water due to swelling. The adhesion of polyimide on other materials, such as silicon, will deteriorate when exposed to the moisture in air.[9,10] Therefore, it will be very helpful to understand the diffusion behavior of water in polyimides.

Diffusion of water in polyimide films has been studied for many years.[11-18] In most of the studies, except that by Numata et al.,[11] only Kapton film or films made of flexible polyimides have been extensively investigated. It is therefore difficult to correlate the diffusion characteristics with the structure of polyimide films. Numata et al. have attempted to correlate the diffusion constants of water in various polyimide films with the film packing coefficient. That correlation does fairly show that diffusion constants decrease with the increase of packing coefficient. However, in their correlation, even with very

* To whom correspondence should be addressed.

Journal of Applied Polymer Science, Vol. 43, 857-875 (1991)
 CCC 0021-8995/91/050857-19$04.00

similar packing coefficients, various different polyimides have exhibited very different diffusion constants. Apparently, besides the packing coefficient, there should be some other factors that will, also, govern the diffusion. Therefore, in this study, the effects of the chemical structure of imide molecule and the morphology of imide film on the diffusion of water in various polyimide films will be discussed.

In this study, a bending-beam technique has been used to in situ monitor the diffusion of water in polyimides. The technique has been used for stress measurement for many years, but was first applied by Berry et al. to study the diffusion behavior of moisture in epoxy.[19] By using this technique, we are able to determine the diffusion mechanism as well as the diffusion constants of water in various polyimides, including a rigid-rod polyimide whose films may be too brittle for other techniques. The details of the corresponding theory are presented in a separate paper.[20] In the following sections, experimental procedures regarding polyamic acid synthesis, bending-beam diffusion specimen preparation and measurement, and X-ray specimen preparation and experiment are described.

EXPERIMENTAL

Materials

The starting materials used in this study are dianhydrides (pyromellitic dianhydride [PMDA] and 3,3′,4,4′-benzophenone tetracarboxylic dianhydride [BPDA]), which were purchased from Chrisken Company, Inc., and diamines (4,4′-oxydianiline [ODA] and *p*-phenylenediamine [PDA]), which were purchased from Tokyo Kasei Kogyo Co., Ltd. The solvent used is *N*-methylpyrrolidone (NMP), which was purchased from Janssen Chimica. These materials were used as received.

Polycondensation of Polyamic Acids

Homopolymers

Homopolymers of PMDA–ODA, PMDA–PDA, and BPDA–PDA polyamic acids were prepared as follows[21]: In a four-neck round-bottle flask equipped with a stirring apparatus and a nitrogen-purging tube, a diamine (ODA or PDA) was dissolved in the NMP solvent. When the diamine had been completely dissolved, an equal-molar amount of dianhydride PMDA or BPDA was added gradually. The reaction proceeded for 5 h with stirring. The entire process was done in a nitrogen atmosphere. The resulting solutions had a solid content of 14 wt %. The molecular structures of the resulted polyamic acids (after cured to solid imides) are shown in Figure 1.

Polyblends

Blends of PMDA–ODA with PMDA–PDA, and PMDA–PDA with BPDA–PDA, were obtained by mixing the polyamic acids. The mixing was done under nitrogen for 5 min. The mixed solutions were then kept frozen before use. Another batch was prepared in the same way, but kept at room temperature for 1 or 3 days before use.

Random Copolymers

Random copolyamic acids of PMDA–ODA/PMDA–PDA and PMDA–PDA/BPDA–PDA were prepared according to the method reported in Refs. 22 and 23. Similarly, two different diamines, ODA/PDA, were together dissolved in the NMP solvent before the addition of PMDA.

Imidization

Solid films of the above-mentioned polyamic acids were prepared by spin-casting the solutions on glass substrates. This was followed with curing by prebaking at 80°C for 0.5 h and then from 80 to 350°C in 5 h and heated at 350°C for 30 min. Though polyimide films of PMDA–ODA or BPDA–PDA could be made at a higher ramp rate, those of PMDA–PDA would be much less fragile if cured slowly. Therefore, the ramp rate was kept low as described

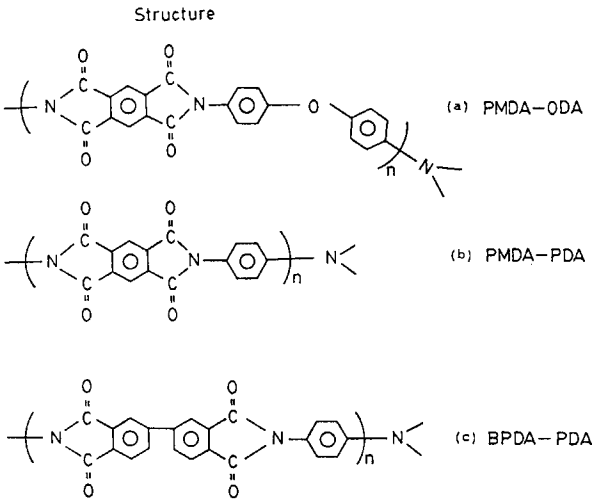

Figure 1 Molecular structures of the studied aromatic polyimides: (a) PMDA–ODA; (b) PMDA–PDA; (c) BPDA–PDA.

above. Since most polyamic acids almost fully imidized at temperatures higher than 300°C, and varying degrees of imidization have an effect on the chain ordering,[24] curing to 350°C seemed adequate.

X-ray Specimen Preparation

The film thicknesses of the polyimide ranged from 4 to 40 μm. In a previous X-ray experiment, it is found that these polyimide films must be thicker than 200 μm so that the X-ray will not penetrate through the films. To compare quantitatively, relatively thick samples are therefore required. This was done by stacking many pieces, e.g., 50 or so, of the films together. By so doing, one has the other advantage of not only structure information in the out-of-plane (film thickness) direction, but also in the in-plane (film plane) direction, being obtained.

X-ray Experiment

X-ray experiments were done using a Rigaku wide-angle X-ray diffractometer with a nickel-filtered copper $K\alpha_1$-radiation. Its power setting was at 40 kV and 20 mA. The line-focus slot has a dimension of 8 × 0.04 mm. The arrangements of the X-ray diffraction experiments are illustrated schematically in Figure 2. For the in-plane diffraction, the sample is so arranged that its film plane is parallel to the plane formed by the incident and reflected beams. For the out-of-plane diffraction, the film plane is perpendicular to the plane formed by the incident and reflected beams. Here, the in-plane direction means the film plane direction and the out-of-plane direction means the film thickness or transverse direction. Since the length of the repeating monomeric units of either one of the two studied polyimides is much larger than the spacing between any two neighboring imide chains, which are usually around 0.4–0.5 nm, one expects to see a characteristic peak. These correspond to "intramolecular" ordering of the former one appearing at a small angle, and those corresponding to the "intermolecular" ordering of the latter one at a large angle, if these polymers are more or less crystalline. One important point should be kept in mind. If a given film is isotropic or has no orientation, its in-plane and out-of-plane diffraction patterns will be the same. Conversely, differences existing between the in-plane and out-of-plane patterns shall indicate structure anisotropy or orientation. If polymeric chains of the studied film are preferably aligned in the plane direction, the intensity of the peak that corresponds to intramolecular ordering should be somewhat higher in the in-plane pattern than in the out-of-plane pattern. Likewise, the intensity of the peak that corresponds to intermolecular ordering should be somehow lower in the in-plane pattern than in the out-of-plane pattern.

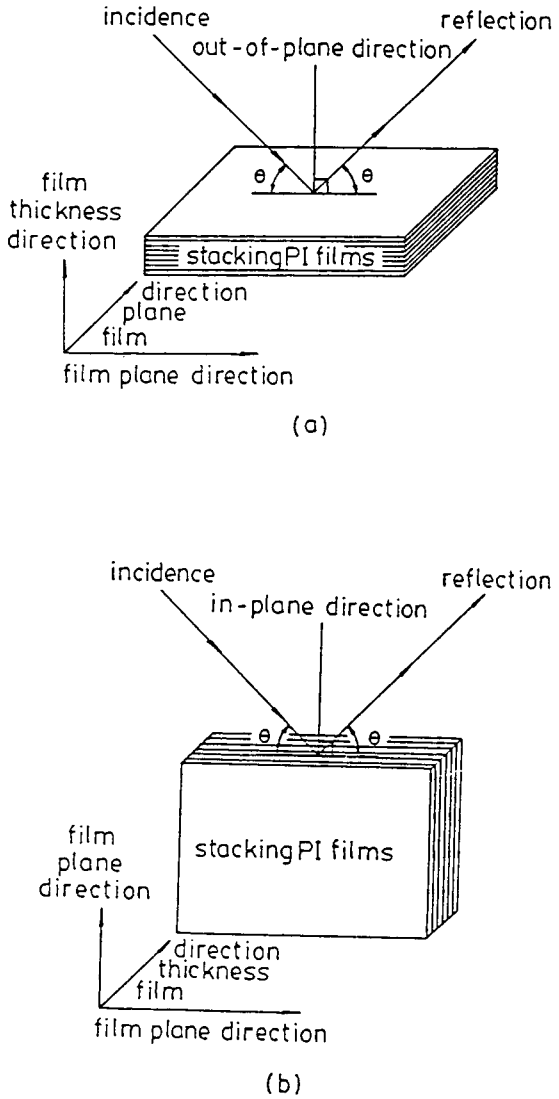

Figure 2 Schematic illustration of the arrangement of the X-ray diffraction experiment: (a) the out-of-plane diffraction, in which the sample is so arranged that its film plane is perpendicular to the plane formed by the incident and reflected beams; (b) the in-plane diffraction, in which its film plane is parallel to the plane formed by the incident and reflected beams.

Bending-beam Specimen Preparation

The substrates used for stress measurement are a silicon strip of 7.5 cm in length, 0.5 cm in width, and 390 μm in thickness. These silicon strips were

prepared by slicing (100) silicon wafers along the (100) crystal plane. Polyimide films were prepared by spin-casting their polyamic acid solutions on the substrates, followed by prebaking at 80°C for 30 min, and then cured from 80 to 350°C at a rate of 1°C/min. During the prebake, part of the solvent is removed in order to solidify the film. Since one end of the substrate must be mounted on a clamp and the other end must reflect the laser beam to a sensor, the two ends of the solid film were removed by 1 cm.

Bending-beam Experiment

Figure 3 shows a schematic diagram of the experiment setup for the in situ bending-beam experiment. Before being measured, the specimen was dried at 120°C for 1 h in a vacuum chamber. The specimen was mounted on a clamp. Before immersing the specimen in water, a drier is used to dry the surface of the specimen. A nitrogen purge is used to cool off and prevent moisture uptake of the film. The deflection of the end of a specimen was measured continuously by a computer-controlled system during the measurement. The change in the deflection was detected by a position-sensitive detector. The measured analog signals were amplified and transformed to digital signals by a signal processor. The processed signals were then transferred via a multioperation signal switch to a data acquisition system. The data acquisition system consisted of a PC/AT and a 14 bits A/D + D/A + DIO control card. After calculation, the obtained position data were converted to bending curvature, $1/R$, according to the geometry of the setup.

Stress in the polyimide film can be readily calculated from the bending curvature, $1/R$, according to the following equation[25]:

$$\sigma_{2,r} = \frac{1}{6R} \frac{E_1}{(1 - \nu_1)} \frac{d_1^3}{d_2(d_1 + d_2)} \quad (1)$$

where $\sigma_{2,r}$ is the average stress in the polymer film; R is the curvature radius of the specimen; E_1, ν_1, and d_1 are Young's modulus, Poission's ratio, and thickness of the substrate, respectively; and d_2 is the thickness of the polymer film.

In the above equation, it has been assumed that the tensile modulus of the polyimide film is much smaller than the Young's modulus of the silicon substrate. A more simplified formula can be reached if the thickness of the polyimide film is comparatively small.[26] However, in this stress experiment, the film thickness ranges from 4 to 40 μm and the thickness of the silicon substrate is 390 μm. The calculated stresses will be overestimated by ranging from 1.0 to 7.8% if the oversimplified formula is applied. To investigate the effect of coating thickness on the resulting stress more precisely, the oversimplified formula is avoided. Instead, eq. (1) is used for stress calculation.

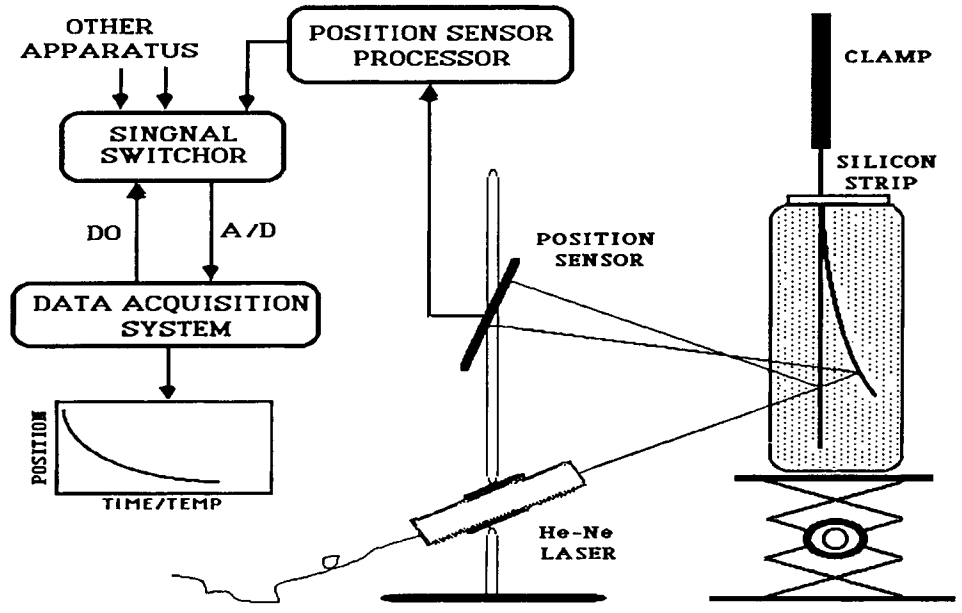

Figure 3 Schematic diagram of the experiment setup for in situ diffusion measurement using a bending-beam apparatus.

RESULTS AND DISCUSSION

Diffusion Mechanism

For the 6.7 μm PMDA–ODA film, the curvature variation ratio ψ, measured in situ by the bending-beam apparatus, is shown in Figure 4(a). The theoretical solid curve is obtained by assuming the diffusion mechanism of water in the film is Fickian with a diffusion constant of 4.9×10^{-9} cm^2/s. As seen, the Fickian diffusion curve well fits the experimental data.

For a thicker PMDA–ODA film, i.e., 11.4 μm, the theoretical curve with a diffusion constant of 5.6×10^{-9} cm^2/s fits the experimental data fairly well, as shown in Figure 4(b). From these results, it can be said that the diffusion of water in the PMDA–ODA films obeys Fick's law or belongs to Case I.

For the PMDA–ODA film with thickness of 18.7 μm, the theoretical curve with a diffusion constants of 4.9×10^{-9} cm^2/s also well fit the experimental data except at the initial stage. In this calculation, a 2 s induction time is used for best-curve fitting.

For the PMDA–ODA film with thicknesses of 19.2 and 27.3 μm, their theoretical curves with diffusion constants of 5.5 and 5.6×10^{-9} cm^2/s, respectively, also well fit the corresponding experimental data except at the initial and near the equilibrium stages. For the 19.2 μm PMDA–ODA film, a 1.5 s induction time is used in the curve fitting. For the 27.3 μm PMDA–ODA film, a 6 s induction time is used in the curve fitting. At near equilibrium, the experimental data in both of these two results deviate from the Fickian diffusion curves.

There exists no clear relationship between the induction times and the film thicknesses. The average induction time in the PMDA–ODA films seems to be very small. The induction behavior can take a certain period of time, though relatively short here, for the film surface to reach a constant concentration before diffusion effectively occurs.[27]

As to the deviations in the final stage, it can be attributed to nonuniformity of the film surface. The films, though prepared by spin-coating, exhibit bumps at their edges due to surface tension. Figure 5 illustrates schematically the bumps in a film that coated on a silicon strip in the width direction. The polyimide films were coated on silicon strips with dimensions of 0.8 cm in width and 7.0 cm in length. The bumps as measured have widths ranging from 0.5 to 1 mm. The bumps in the length direction can be ignored since they locate very near the edges and have been removed for clamping and reflecting the laser beam in the bending-beam experiment, as mentioned in the Experimental section. However, as shown in Figure 5, the bumps in the width direction cannot always be ignored since they may occupy nearly $\frac{1}{8}$ to $\frac{1}{4}$ of the total width. The height of the bump, d(maximum), as shown in the plot, may be two times of the thickness of the film at center, d(minimum), or up to $\frac{8}{5}$ to $\frac{16}{9}$ of the mean thickness, d(mean). Consequently, it would take a much longer period of time for water to diffuse and reach a constant equilibrium concentration at which the bump is located. Ideally speaking, the time needed for such a nonuniform film to reach equilibrium is proportional to the square of the ratio of d(maximum)/d(mean) in case of Fickian diffusion. In these bending-beam diffusion experiments, the deflection positions of the specimens, instead of the diffusion times at equilibrium, are required for the calculation of diffusion constants. The effect of nonuniformity in the film thickness is negligible.

Furthermore, as learned from a previous computation by using a finite element method, the deflection of a given substrate caused by a nonuniform film like that in Figure 5 is the same as caused by an uniform film with a thickness equal to the mean thickness of the nonuniform film. Therefore, once the equilibrium deflection position of a given specimen is measured, it can be used to calculate the desired diffusion constant.

As to where the experimental data should start to deviate from the Fickian diffusion curve due to film nonuniformity depends on the relative magnitude of d(minimum)/d(mean). As one can imagine, after a certain period of diffusion time and before equilibrium, the thinner portion of the film, i.e., with a thickness of d(minimum), may have reached equilibrium while the rest of the film has not. The equilibrium portion would then cease but the rest would keep on causing deflection change. Unlike in the initial stage, the deflection variation with respect to time would then be lessened due to less area available for diffusion. When this happens, experimental data starts to deviate from the Fickian diffusion curve. If the film prepared were extremely flat, i.e., d(minimum)/d(mean) is very near unity, there should be no deviation or the deviation should occur at a relatively late time period or at a curvature variation ratio ψ that is very near one. Conversely, the experimental data would have deviated from the Fickian diffusion curve at a much earlier time period or at a smaller curvature variation ratio ψ if d(minimum)/d(mean) were much smaller than 1. In these experiments, the ratios of d(minimum)/d(mean) in various films are around 0.7–0.9. However, further experiments are required to quantitatively investigate these deviations.

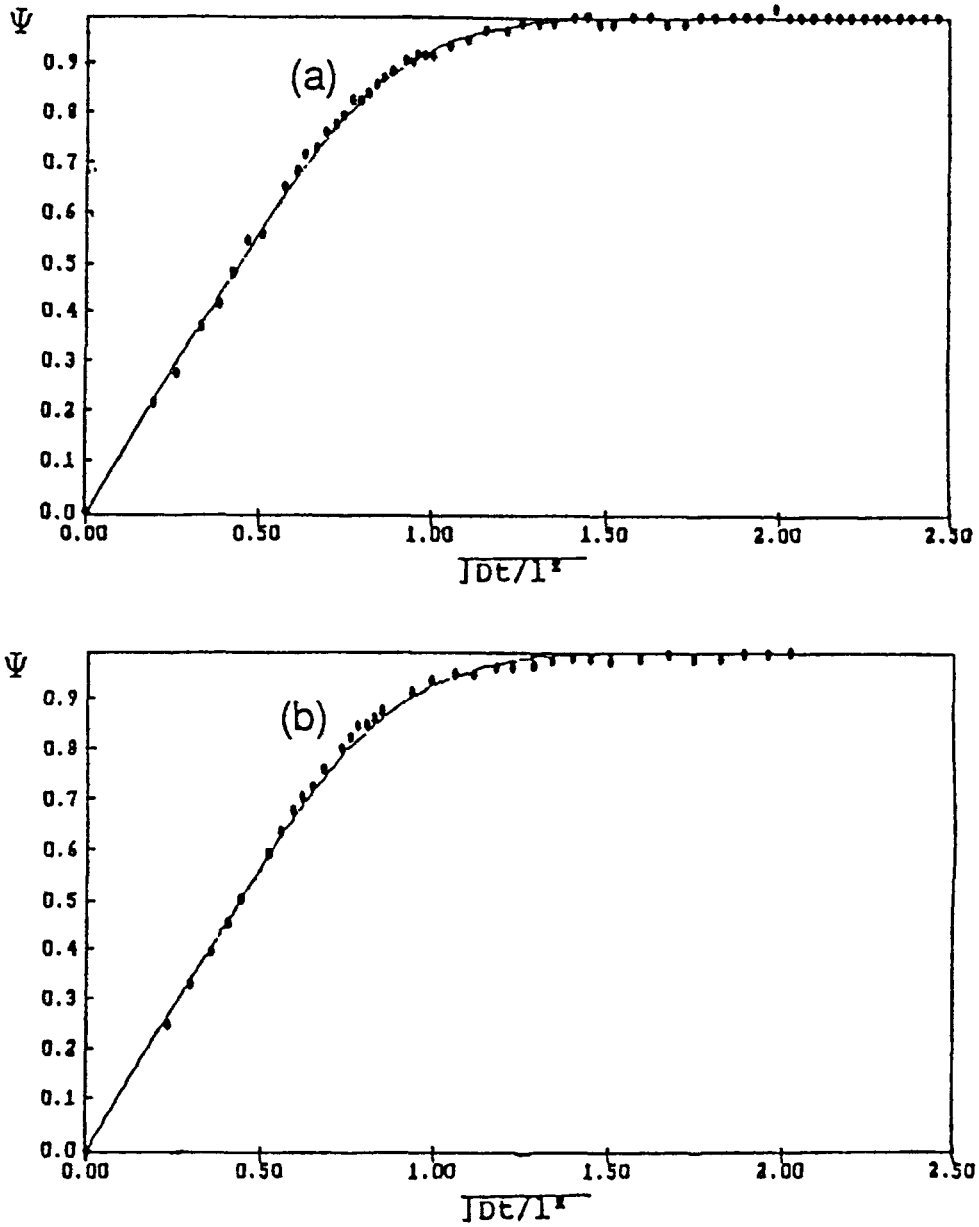

Figure 4 The relationship between the curvature variation ratio ψ and $(Dt/l^2)^{1/2}$ for diffusion of water in PMDA–ODA film with different thicknesses: (a) 6.7 μm; (b) 11.4 μm; (c) 18.7 μm; (d) 19.2 μm; (e) 27.3 μm. The solid curves are obtained by assuming that the diffusion mechanism of water in the films is Fickian. (D: diffusion coefficient; t: diffusion time; 1: film thickness.)

Diffusion in Rodlike Polyimides

The diffusions of water in several PMDA–PDA films are shown in Figure 6(a)–(e). The film thicknesses range from 7.3 to 20.0 μm. From the thinnest to the thickest, the diffusion constants of water in these rigid rodlike PMDA–PDA films are 1.1, 1.8, 2.8, 1.8, and 2.3×10^{-9} cm^2/s, respectively. These diffusion constants are much smaller than those in PMDA–ODA films. It may be attributed to differences in their chemical structures and/or their morphologies. By comparing the chemical structures of PMDA–PDA and PMDA–ODA, one can attribute the faster diffusion of water in the films of PMDA–ODA to the presence of the —O— ether linkage. The ether linkage can be treated as a diffusion favorable site since it is hydrophilic.

As revealed by the X-ray diffraction patterns, the

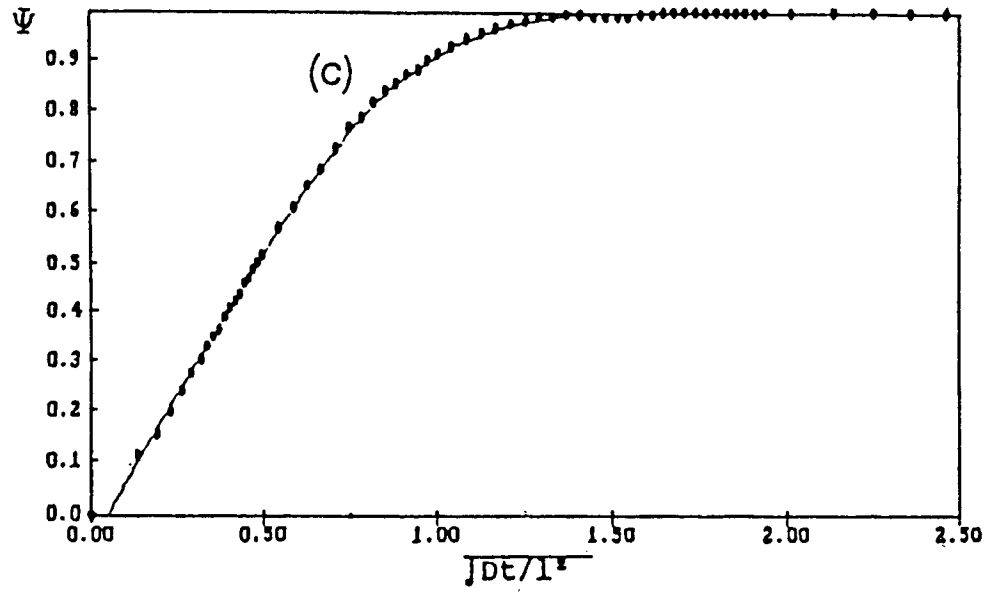

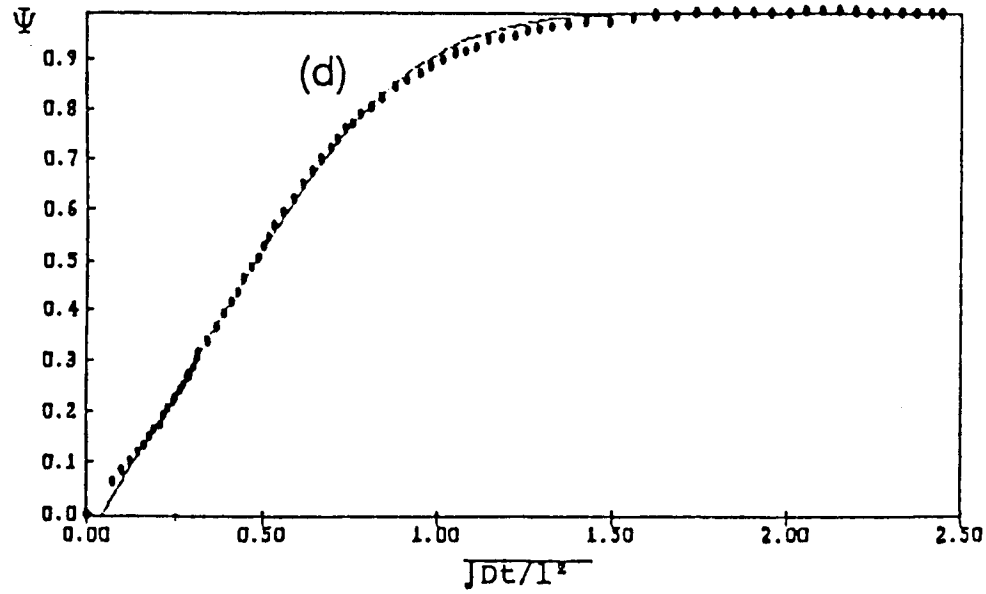

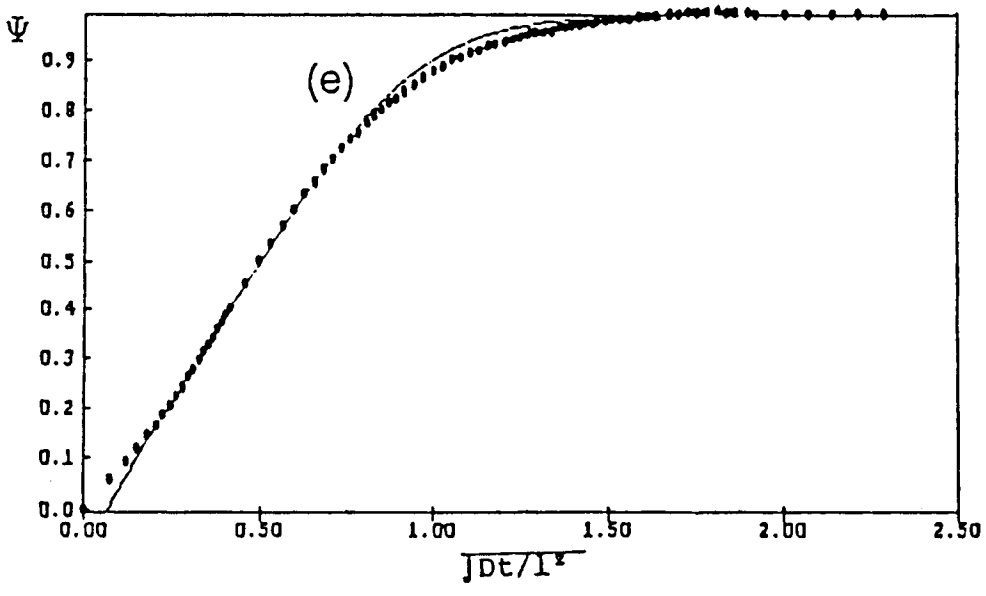

Figure 4 (*Continued from the previous page*)

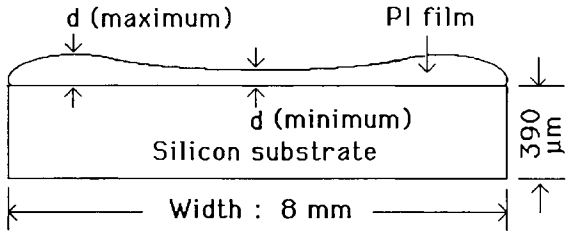

Figure 5 Schematic illustration of the bumps at the edges of a typical spin-cast polyimide film after curing.

on-substrate-cured PMDA–PDA films are relatively highly crystalline, while the PMDA–ODA films are relatively amorphous.[28] From this standpoint, one can also attribute the smaller diffusion constants in the PMDA–PDA films to the higher crystallinity. However, from the above results, it is still difficult to distinguish whether the chemical nature of the structure unit or the film crystallinity has played a more important role in affecting the diffusion of water.

The diffusions of water in BPDA–PDA films are shown in Figure 7(a)–(e). The film thicknesses range from 4.8 to 21.0 μm. From the thinnest to the thickest, the diffusion constants of water in these rigid rodlike BPDA–PDA films are 0.29, 0.23, 0.28, 0.28, and 0.27×10^{-9} cm^2/s, respectively. These diffusion constants are much smaller than those in the PMDA–ODA films. They are about an order smaller than those in the PMDA–PDA films. As demonstrated by their out-of-plane X-ray diffraction patterns in Figure 8, the BPDA–PDA films do not exhibit higher crystallinity than do the PMDA–PDA films. As also indicated in the paper,[11] the packing coefficients of the films of PMDA–PDA and BPDA–PDA are very similar to each other. In these two rigid rodlike films, i.e., PMDA–PDA and BPDA–PDA, the significant difference between their diffusion constants, therefore, cannot be attributed to the difference in their crystallinities or packing coefficients. On the contrary, it should be attributed to the difference between the chemical natures of the structure units of the two different polyimides. Both of these two imides have the same PDA component. The only difference exists between the PMDA and BPDA components. In BPDA, it composes a hydrophobic 3,3′,4,4′-biphenylene group, which contains two benzene structure units, whereas in PMDA, the 1,2,4,5-phenylene group contains only one benzene structure unit. As a water diffusion barrier, a larger hydrophobic group, such as 3,3′,4,4′-biphenylene, seems to be more effective than is a smaller one, such as 1,2,4,5-phenylene. Consequently, the diffusion of water in the film of BPDA–PDA would be greatly inhibited.

Similar to PMDA–ODA, the experimental curves of the diffusion of water in the PMDA–PDA and BPDA–DPA films deviate from the corresponding theoretical Fickian curves at near equilibrium. The induction times in the PMDA–PDA films are relatively short. They can be barely observed. In the BPDA–PDA films, the induction times are relatively long and range from 10 to 45 s. This perhaps can also be attributed to the effect of the 3,3′,4,4′-biphenylene group.

Diffusion in Blends and Random Copolymers

The effects of chemical structure and morphology on diffusion have been further examined by measuring the diffusion of water in the blends of the above-mentioned polyimides. By so doing, one may be able to distinguish whether chemical structure or morphology, such as crystallinity, has played a more significant role in affecting the diffusion of water in those imide films.

The diffusions of water in the imide films of the various polyimides with PMDA–ODA and PMDA–PDA are shown in Figure 9(a)–(e). Figure 9(b) shows that the blend with 50% PMDA–ODA and 50% PMDA–PDA was obtained by mixing their precursor solutions for 5 min before cured to imide. The film thicknesses range from 9.6 to 21.6 μm. From the thinnest to the thickest, the diffusion constants of water in these films are 4.0, 3.9, 4.1, 4.2, and 3.3×10^{-9} cm^2/s, respectively. These diffusion constants are slightly smaller than those in the pure PMDA–ODA films, but much larger than those in the pure PMDA–PDA films.

When the blend has been mixed for a much longer period of time, i.e., 1 day, the diffusion constants slightly increase. Figure 9(c) shows the diffusion of water in the films of this blend. The film thicknesses range from 5.0 to 35.8 μm. From the thinnest to the thickest, the diffusion constants are 4.7, 5.5, 4.9, 4.0, 4.3, and 5.0×10^{-9} cm^2/s, respectively.

Figure 9(d) shows the diffusion of water in the films of the corresponding random copolymer with 50% PMDA–ODA and 50% PMDA–PDA. The film thicknesses range from 8.2 to 43.2 μm. From the thinnest to the thickest, the diffusion constants are 5.7, 5.0, 3.8, 3.6, 2.8, and 3.3×10^{-9} cm^2/s, respectively. When compared, the diffusion constants in these random copolymer films are nearly equal to those in the films of the blend mixed for 1 day, especially in the thickness range from 10 to 20 μm. Apparently, the blend after mixing for a long period

of time has converted to a random copolymer from this standpoint. As also reported in the paper by Jou et al.,[28] the blend of any two polyamic acids would eventually convert to a random copolymer because of the exchange reaction.

Figure 10 compares the out-of-plane X-ray diffraction patterns of the 50% PMDA–ODA and 50% PMDA–PDA films of the laminate, the blend mixed for 5 min, the blend mixed for 1 day, and the random copolymer. As indicated by the (a) and (f) patterns, the pure PMDA–PDA film is relatively crystalline, whereas the pure PMDA–ODA film is amorphous. The diffraction pattern of their laminate has a peak intensity exactly proportional to the extent of PMDA–PDA, as seen in curve (b). The diffraction pattern of the blend mixed for 5 min, as shown by curve (c), has a peak height slightly smaller than that of the laminate. Furthermore, its peak is much broader. This indicates that the two imides in the blend start mixing in 5 min. The reduction in the peak intensity can be attributed to partial destruction of the ordering structure of the imides of PMDA–PDA caused by the intervening of the flexible imide chains of PMDA–ODA due to intermixing or exchange reaction. When mixed for a much longer time period, for example, 1 day, the characteristic peak significantly drops. Its diffraction pattern, curve (e), becomes extremely similar to that of the random copolymer, curve (d). It seems that the blend has already converted to a random copolymer. From the results shown above, it can be seen that the diffusion constants depend much more on the chemical structure than on the morphology.

For the blend with 50% BPDA–PDA and 50% PMDA–PDA and mixed for 5 min, the diffusions of water in the imide films are shown in Figure 11(a)–(e). The film thicknesses range from 4.6 to 18.2 μm. From the thinnest to the thickest, the diffusion constants of water in these films are 0.35, 0.30, 0.35, 0.35, and 0.27×10^{-9} cm^2/s, respectively. These diffusion constants are much smaller than those in the pure PMDA–PDA films, but very close to those in the pure BPDA–PDA films.

For the blend that has been mixed for 3 days, the diffusion constants increase, but are still very close to those in the pure BPDA–PDA films. Figure 11(c) shows the diffusion of water in the films of this blend. The film thicknesses range from 4.7 to 24.0 μm. From the thinnest to the thickest, the diffusion constants are 0.70, 0.51, 0.38, 0.36, and 0.36×10^{-9} cm^2/s, respectively.

Figure 11(b) shows the diffusions of water in the films of the random copolymer with 50% BPDA–PDA and 50% PMDA–PDA. The film thicknesses range from 3.0 to 23.4 μm. From the thinnest to the thickest, the diffusion constants are 0.45, 0.95, 0.79, 0.40, and 0.45×10^{-9} cm^2/s, respectively. When compared, the diffusion constants in these random copolymer films are relatively small and very different from those in the pure PMDA–PDA films, especially in the thickness range from 10 to 20 μm. The diffusion in the PMDA–PDA film has been drastically reduced by the presence of BPDA–PDA. This should be attributed to the diffusion-unfavorable 3,3′,4,4′-biphenylene group. It seems that the morphology of these films is a secondary factor.

Figure 12 compares the out-of-plane X-ray diffraction patterns of the 50% BPDA–PDA and 50% PMDA–PDA films of the blend mixed for 5 min, the blend mixed for 3 days, and the random copolymer. As indicated by the (a) and (b) patterns, the pure BPDA–PDA film is crystalline, but somewhat less ordered than is the pure PMDA–PDA film. This is reasonable since BPDA has a less symmetrical molecular structure in comparison to PMDA. The diffraction pattern of the blend mixed for 5 min, as shown by curve (c), clearly indicates that it is compatible. Originally, pure BPDA–PDA had two diffraction peaks. The first peak appears at a smaller angle, where the major characteristic diffraction peak appears. The second peak appears at a larger angle. When blended with PMDA–PDA, the second peak almost disappears. Besides, the first peak of the blend has an intensity smaller than those of the two pure polyimides. If the blend was incompatible, the first peak should have had an intensity, with respect to composition, equal to that superimposed by those of the two pure imide peaks and its intensity should have been higher than that of the pure BPDA–PDA. It can be concluded that this blend that only mixed for 5 min is compatible. Similarly, the reduction in the peak intensities can be attributed to destruction of the ordering structures of the two imides caused by the cross-intervening of their dissimilar imide chains upon intermixing or exchange reaction. For the blend mixed for 3 days, the first characteristic peak drops further. This blend seems to be more completely compatible.

Though the structure ordering of the films of this blend has been significantly destroyed due to its compatibility, the diffusion of water in these films has not been enhanced. Their diffusion constants are still as small as those in the pure BPDA–PDA films. It seems that the film crystallinity is merely a secondary factor. The major factor in determining the magnitude of the diffusion constant of water in these films should be the chemical structure of the imides.

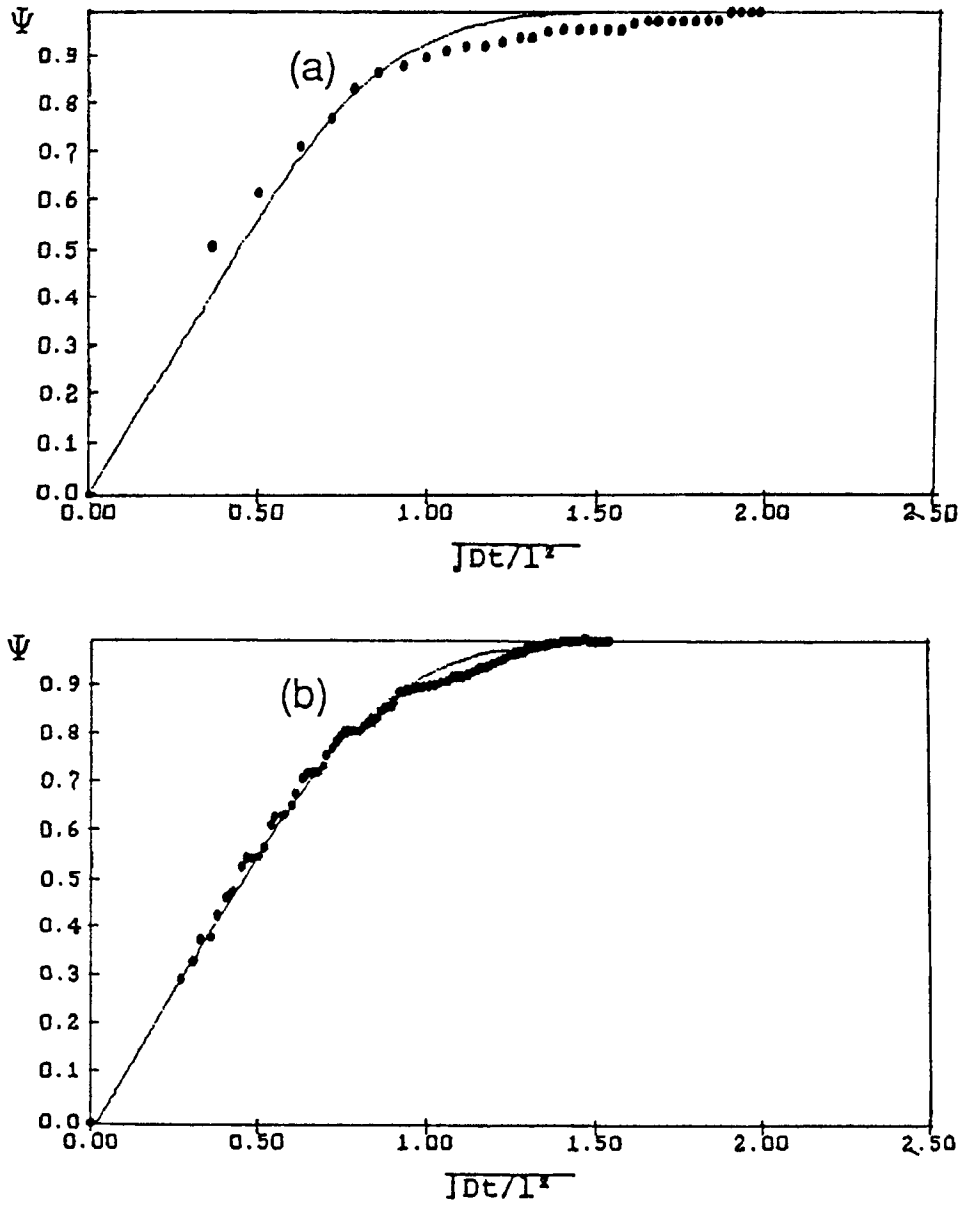

Figure 6 The relationship between the curvature variation ratio ψ and $(Dt/l^2)^{1/2}$ for diffusion of water in PMDA–PDA film with different thicknesses: (a) 7.3 μm; (b) 11.0 μm; (c) 15.0 μm; (d) 17.4 μm; (e) 20.0 μm.

Hygroscopic Stress

Generally, polyimide films cured on substrate always exhibit internal stress.[29,30] The stresses in the films may be tensile or compressive. It depends on their thermal expansion coefficients and the substrate and on the condition of curing process. Whether the internal stress in a given film is tensile or compressive, when uptaking water, it will more or less swell. Such a swelling in the film will have a compressive effect on itself. If the film is originally in a tensile state, it will become less tensile or even compressive. If it is in a compressive state, it will become more compressive. The stress that arises due to water or solvent uptake is called hygroscopic stress. The hygroscopic stress can be determined by measuring the stress difference upon diffusion.

Figure 13 shows relationship of the hygroscopic stresses in the PMDA–ODA films with film thickness. The stress at equilibrium is defined as the hygroscopic stress. As seen, the thinner films have less hygroscopic stress. The hygroscopic stresses in these films range from 1.3 to 2.0 kpsi. They correspond to hygroscopic strains of 0.0021 to 0.0032, based on

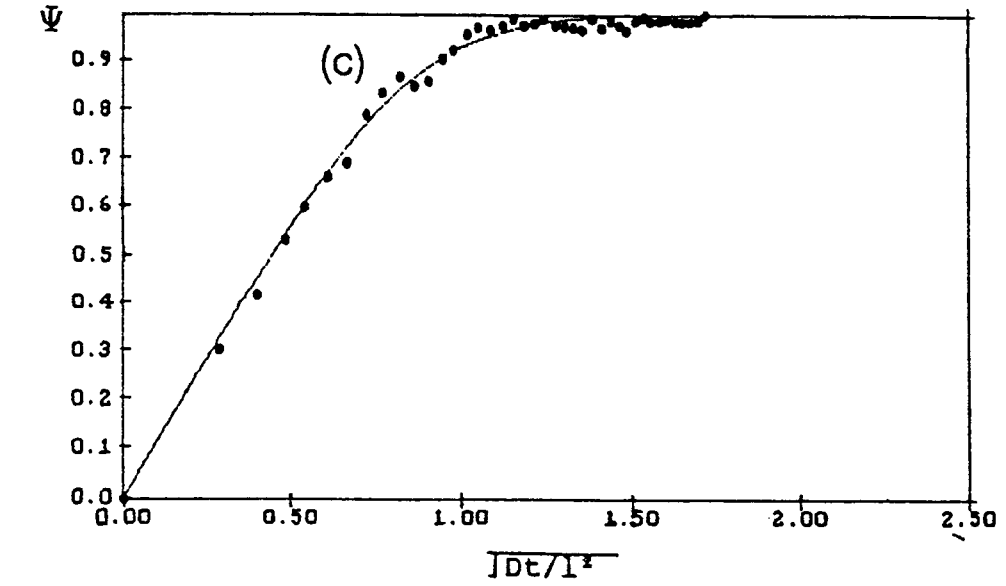

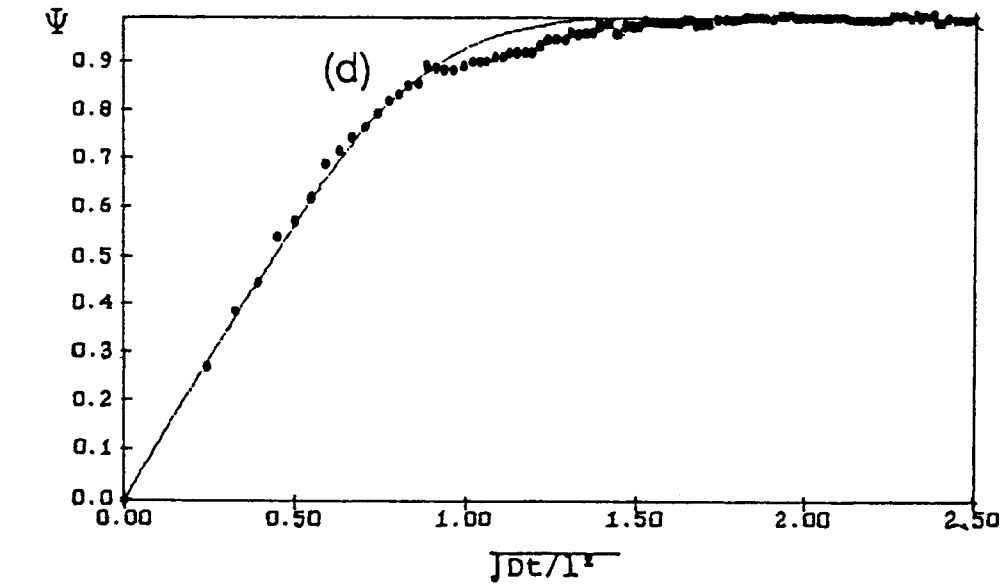

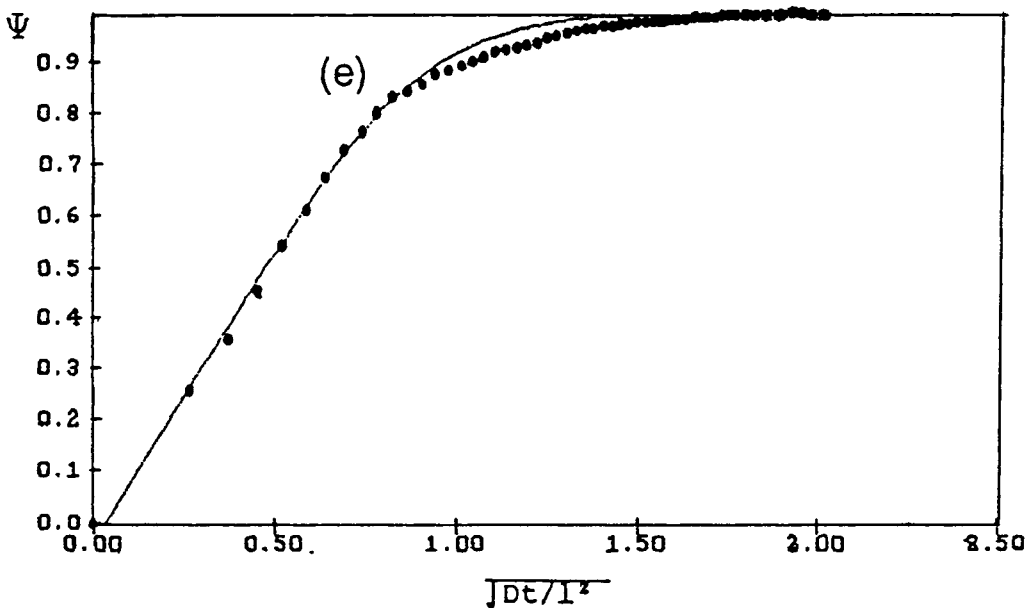

Figure 6 (*Continued from the previous page*)

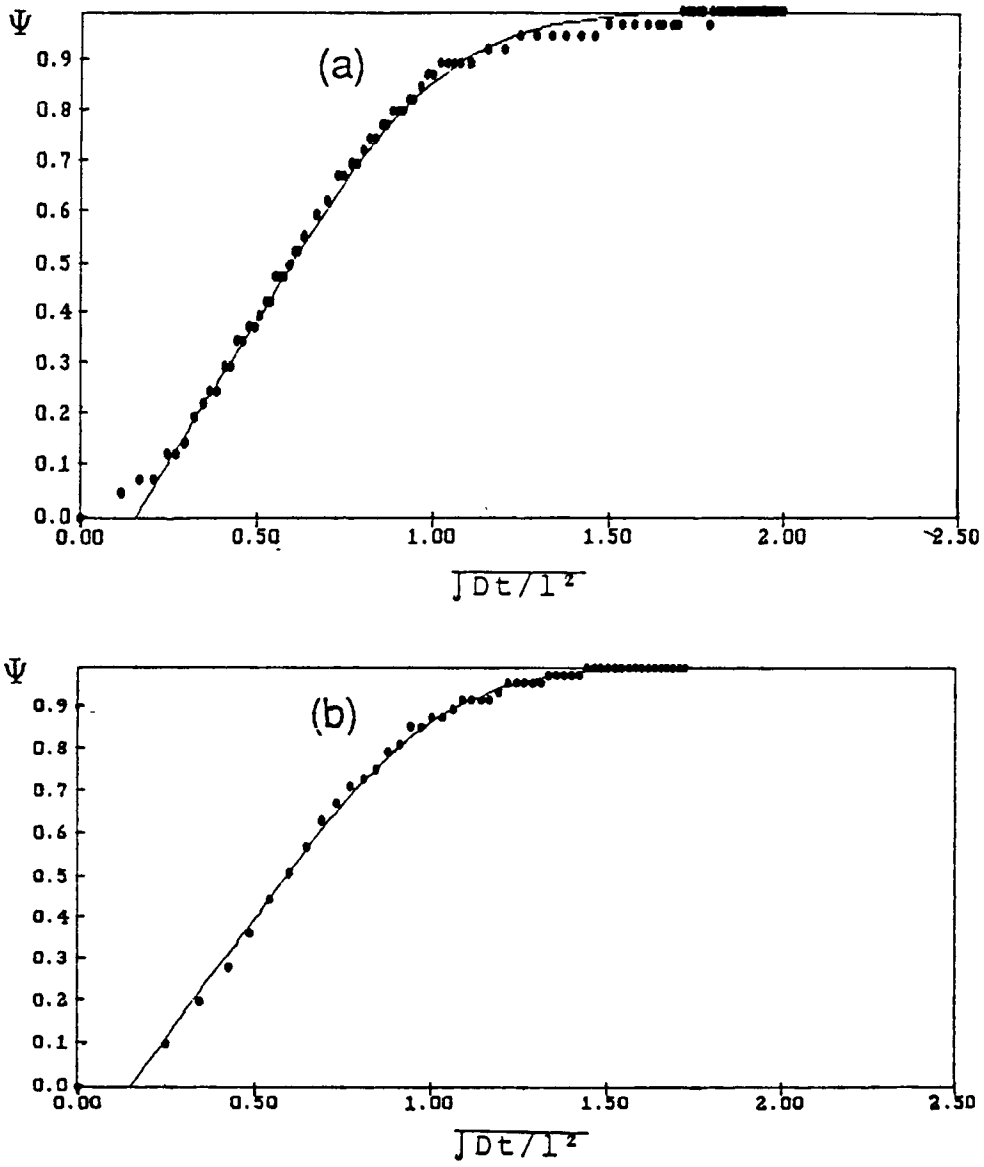

Figure 7 The relationship between the curvature variation ratio ψ and $(Dt/l^2)^{1/2}$ for diffusion of water in BPDA–PDA film with different thicknesses: (a) 4.8 μm; (b) 6.8 μm; (c) 10.4 μm; (d) 15.5 μm; (e) 21.0 μm.

their relaxation moduli of 340 kpsi and Poisson ratio of 0.47.

Figure 14 shows relationship of the hygroscopic stresses in the PMDA–PDA films with film thickness. The thinnest film has the least hygroscopic stress. For those thicker films, the hygroscopic stresses slightly decrease with the increase of film thickness. However, they are comparatively larger than that of the thinnest film. As listed in Table I, from 7.3 to 20.0 μm, the hygroscopic stresses range from 3.0 to 5.0 kpsi. They correspond to hygroscopic strains of 0.0011 to 0.0018, based on their relaxation moduli of 1400 kpsi.

Figure 15 shows relationship of the hygroscopic stresses in the BPDA–PDA films with film thickness. Similarly, the thinner films have less hygroscopic stress. As listed in Table I, from 4.8 to 24.4 μm, the hygroscopic stresses range from 1.1 to 1.8 kpsi. They correspond to hygroscopic strains of 0.0005 to 0.0008, based on their relaxation moduli of 1280 kpsi.

Table I summarizes all the hygroscopic stresses and strains in the studied films. Within the studied

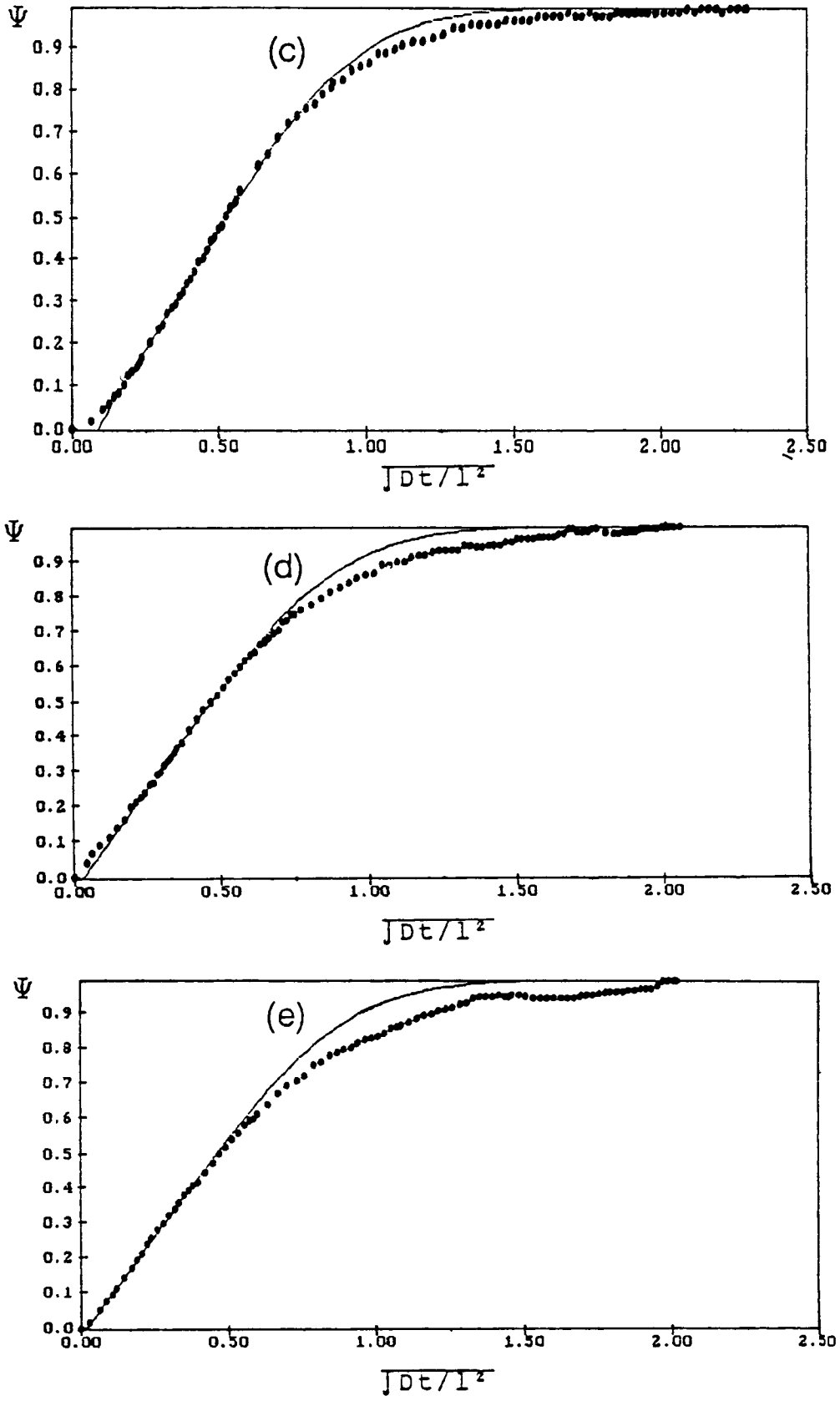

Figure 7 *(Continued from the previous page)*

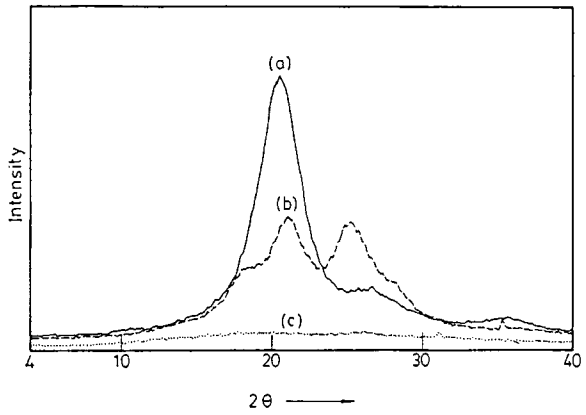

Figure 8 Out-of-plane X-ray diffraction patterns of the stacked polyimide films of (a) PMDA–PDA, (b) BPDA–PDA, and (c) PMDA–ODA.

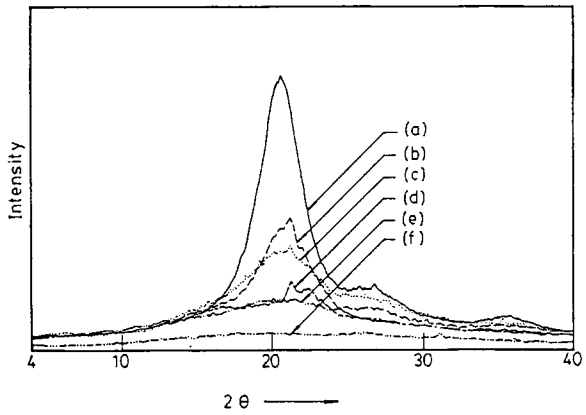

Figure 10 Out-of-plane X-ray diffraction patterns of the stacked polyimide films of (a) the pure PMDA–PDA, (b) the laminate, (c) the blend mixed for 5 min, (d) the random copolymer, (e) the blend mixed for 1 day, and (f) the pure PMDA–ODA. (c)–(e) are polyimides with 50% PMDA–ODA and 50% PMDA–PDA.

thickness range, hygroscopic stresses in the blends with 50% PMDA–ODA and 50% PMDA–PDA increase with the increase of thickness, regardless of the mixing time or morphology. The hygroscopic stress approaches an asymptotic value at about 30 μm. For pure PMDA–ODA, the asymptotic value appears at about 20 μm, and for pure PMDA–PDA, at 11 μm. Similarly, hygroscopic stresses in the blends with 50% BPDA–PDA and 50% PMDA–PDA increase with the increase of thickness. But no asymptotic value has been observed for all samples containing BPDA–PDA.

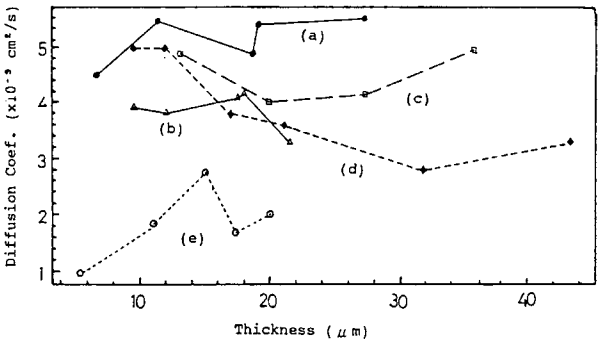

Figure 9 The relationship between diffusion coefficients of water in various imide films and film thickness: (a) pure PMDA–ODA; (b) blend with 50% PMDA–ODA and 50% PMDA–PDA obtained by mixing their precursor solutions for 5 min before being cured to imide; (c) blend with 50% PMDA–ODA and 50% PMDA–PDA obtained by mixing their precursor solutions for 1 day before being cured to imide; (d) random copolymer with 50% PMDA–ODA and 50% PMDA–PDA; (e) pure PMDA–PDA.

The above phenomena may be attributed to film orientation. As presented in a separate paper,[31] the film orientation strongly depends on coating thickness. It decreases as the film thickness increases. To demonstrate, Figure 16 shows the in-plane X-ray diffraction patterns of the films of BPDA–PDA with various thicknesses. It can be seen that the peak at $2\theta = 11°$, which corresponds to the spacing of the imide repeating units, is decreasing with thickness, while those near $2\theta = 24$–$30°$, which correspond to the interchain spacings, remain nearly unchanged. This indicates that fewer and fewer imide repeating units have been seen preferably aligning parallel to the film plane when the thickness increases. One can conclude that the film orientation decreases with thickness.

Why the hygroscopic stress increases with the decrease of the film orientation is thought to be as follows: As just demonstrated, the films with higher degrees of orientation have more imide chains aligning in the film plane direction. If a film has a perfect orientation, i.e., all imide chains are aligning in the film direction, it will be more difficult to deform it from a direction parallel to the film than by transversing the film. In the parallel direction, the major resistance to deformation is from the intramolecular covalent bonds, whose bond forces are much stronger than are the intermolecular forces existing in the transversing direction. Actually, this thought is not new. Most oriented polymers or fiber-reinforced composites are more resistant to defor-

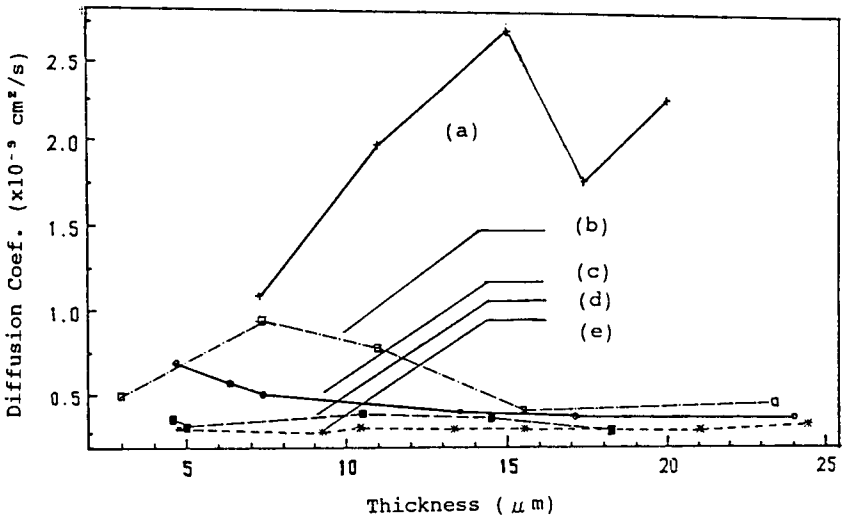

Figure 11 The relationship between diffusion coefficients of water in various imide films and film thickness for different polyimides: (a) pure PMDA–PDA; (b) random copolymer with 50% PMDA–PDA and 50% BPDA–PDA; (c) blend with 50% PMDA–PDA and 50% BPDA–PDA obtained by mixing their precursor solutions for 3 days before being cured to imide; (d) blend with 50% PMDA–PDA and 50% BPDA–PDA obtained by mixing their precursor solutions for 5 min before being cured to imide; (e) pure BPDA–PDA.

mation in the oriented or reinforced direction. Similarly, when the films swell upon uptaking water, they would swell more in the transverse direction and less in the film plane direction. From another aspect, they would swell anisotropically, as indicated in the paper by Gattiglia et al.,[32] though the swelling experiments have been done in solvents. In this study, the change in the dimensions of all the studied films upon water sorption cannot be directly measured due to the uptake amount of low water uptake,

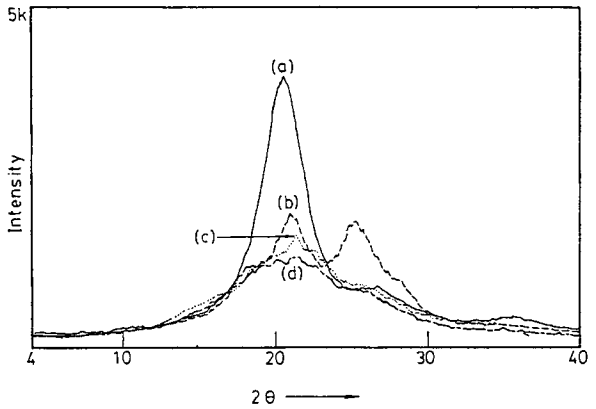

Figure 12 Out-of-plane X-ray diffraction patterns of the stacked polyimide films of (a) the pure PMDA–PDA, (b) the pure BPDA–PDA, (c) the blend mixed for 5 min, and (d) the blend mixed for 3 days.

namely, < 3 wt %. Besides, water is a nonsolvent to polyimide. It would not cause much swelling.

Since the thicker films have a poor orientation, they have comparatively less imide chains aligning parallel to the film and can swell more in the film plane direction. As a result, the thicker films exhibit higher hygroscopic stress or strain. As to the asymptotic phenomenon, it may be attributed to that the film orientation would not further decrease above a coating thickness, which seems to depend on the type of polyimide and curing process.

As seen in Table I, hygroscopic strains in the films blended with PMDA–ODA and mixed for 5 min are ranging from 0.0015 to 0.0021, based on their relaxation moduli of 700 kpsi. Since PMDA–PDA films are very brittle, it is extremely difficult to prepare films above 20 μm, except when blended with PMDA–ODA. To compare within the same thickness range, i.e., below 22 μm, they are much smaller than those in the pure PMDA–ODA films, but very close to those in the pure PMDA–PDA films. For the blend mixed for 1 day, the maximum hygroscopic strain is 0.0022 below 22 μm and 0.0027 above 22 μm. For the random copolymer, the maximum hygroscopic strain is 0.0020 below 22 μm and 0.0028 above 22 μm.

Hygroscopic strains in the films blended with BPDA–PDA and mixed for 5 min are almost similar to those in the pure BPDA–PDA films. They range

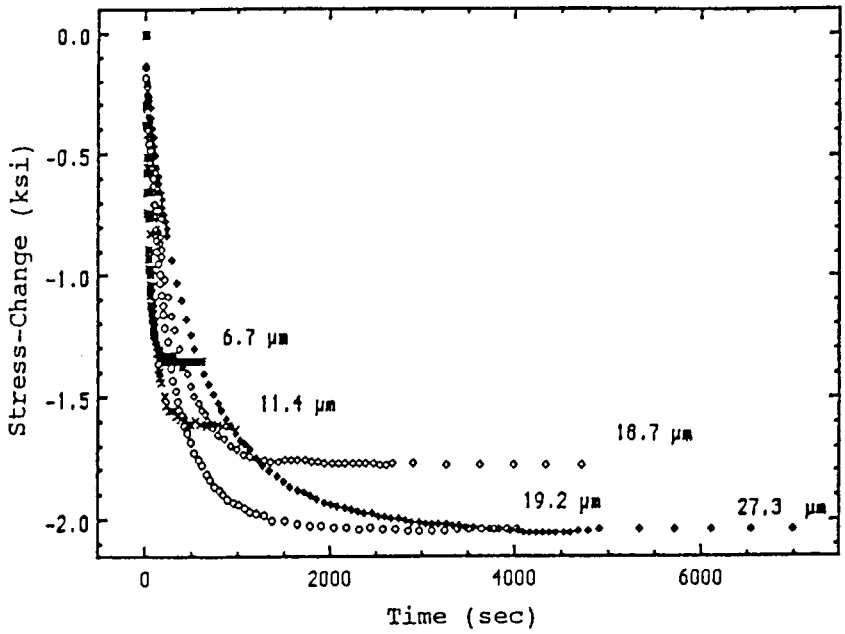

Figure 13 The relationship between the hygroscopic stresses in the PMDA–ODA films and film thickness.

from 0.0005 to 0.0011, based on their relaxation moduli of 1300 kpsi. For the blend mixed for 3 days, the hygroscopic strains are from 0.0003 to 0.0009, while for the random copolymer, from 0.0003 to 0.0009.

As seen, whether in the pure PMDA–PDA, blend, or random copolymer, all the maximum hygroscopic strains are around 0.0021 for thickness below 22 μm. Similarly, for the BPDA–PDA series, the maximum hygroscopic strains are around 0.0012 for thickness

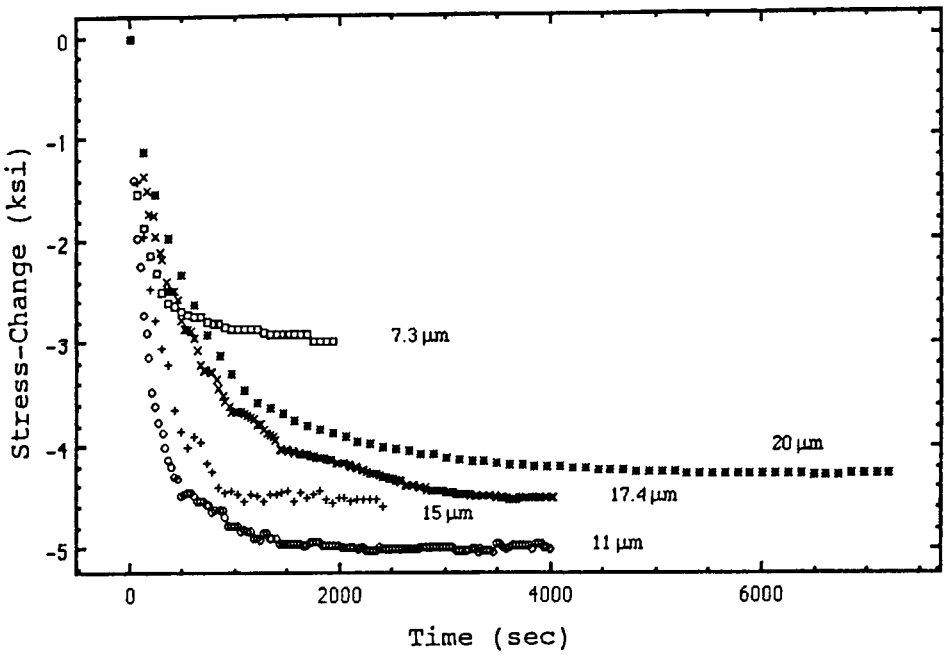

Figure 14 The relationship between the hygroscopic stresses in the PMDA–PDA films and film thickness.

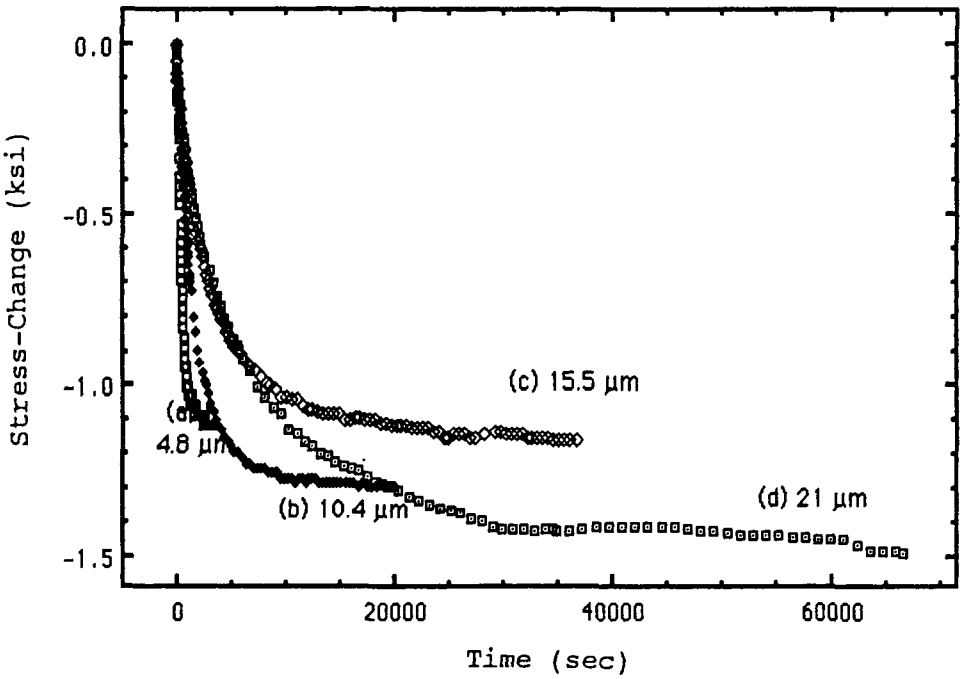

Figure 15 The relationship between the hygroscopic stresses in the BPDA–PDA films and film thickness.

below 25 μm. For the mixtures (blends or random copolymer), providing the water uptake contents are the same, their swelling parameters are nearly the same to one another regardless the difference in their morphologies. These results again indicate that all the blends have readily converted to random copolymers upon mixing.

CONCLUSIONS

A bending-beam technique has been successfully applied to in situ monitor the diffusion of water in various polyimide films. They include a rodlike polyimide, PMDA–PDA, whose films are relatively brittle and have not been studied in other studies by using different techniques.

As demonstrated by the results, the diffusion of water in these films obeys Fick's law, i.e., it is a Case I diffusion. The Case I diffusion occurred after a relatively short period of induction time, which varies with polyimides. The mean induction time for the PMDA–PDA films is the shortest, i.e., around 0.7 s. It is the longest for the BPDA–PDA films and is around 23 s. For the PMDA–ODA films, there is some scattering in the experimental data. It is relatively short and comparable to that for PMDA–PDA.

In the diffusion experiments, various film thicknesses for each polyimide have been used. However, within experimental variation, no specific relationship between diffusion constant and thickness has been observed. In PMDA–ODA, the mean diffusion constant is $5.2 \pm 0.4 \times 10^{-9}$ (cm^2/s) for thicknesses ranging from 6.7 to 27.3 μm. In PMDA–PDA, it is $2.0 \pm 0.4 \times 10^{-9}$ (cm^2/s) for thicknesses ranging from 7.3 to 20.0 μm, and in BPDA–PDA, $0.27 \pm 0.02 \times 10^{-9}$ (cm^2/s) for thicknesses ranging from 4.8 to 21.0 μm.

In the blends and random copolymer with 50 wt % PMDA–ODA and 50 wt % PMDA–PDA, the diffusion constants are slightly smaller than those in the pure PMDA–ODA, but much larger than in the pure PMDA–PDA. On the contrary, those with 50 wt % BPDA–PDA and 50 wt % PMDA–PDA, the diffusion constants are much smaller than those in the pure PMDA–PDA, but slightly larger than those in the pure BPDA–PDA. These diffusion constants are primarily governed by the chemical structure of imide molecule. Morphologies, such as crystallinity, of the films are secondary factors. Hygroscopic stresses due to water uptake in all the studied films increase as the film thickness increases. It can be attributed to that the film orientation decreases with the increase of thickness.

Table I Hygroscopic Stresses and Strains in Various Polyimide (PI) Films

PI Film of	Film Thickness (μm)	Stress (kpsi)	Strain (%)
PMDA–ODA	6.7	1.37	0.21
	11.4	1.69	0.26
	18.7	1.77	0.28
	19.2	2.03	0.32
	27.3	2.04	0.32
PMDA–PDA	7.3	1.40	0.11
	11.0	2.98	0.18
	15.0	4.58	0.17
	17.4	4.50	0.16
	20.0	4.26	0.15
BPDA–PDA	4.8	1.11	0.05
	9.2	1.20	0.05
	10.4	1.28	0.05
	13.3	1.18	0.05
	24.4	1.81	0.08
Blend[a]	9.6	1.92	0.15
(mixed for 5 min)	12.1	2.17	0.16
	17.6	2.49	0.19
	18.2	2.50	0.19
	21.6	2.74	0.21
Blend[a]	5.0	1.08	0.08
(mixed for 1 day)	8.1	1.20	0.09
	11.5	1.69	0.13
	13.2	1.95	0.15
	20.0	2.91	0.22
	27.4	3.66	0.27
Random[a]	9.6	1.24	0.10
copolymer	12.0	1.50	0.11
	17.0	2.18	0.16
	21.1	2.64	0.20
	31.8	3.70	0.28
Blend[b]	4.6	1.16	0.05
(mixed for 5 min)	5.0	1.33	0.05
	6.8	1.50	0.06
	14.5	2.20	0.07
	18.2	2.72	0.11
Blend[b]	4.7	0.33	0.01
(mixed for 3 days)	6.4	0.80	0.03
	10.0	1.12	0.05
	13.5	1.67	0.07
	17.1	2.39	0.10
	24.0	3.50	0.14
Random[b]	3.0	0.75	0.03
copolymer	7.4	0.72	0.03
	11.0	0.92	0.04
	15.5	1.10	0.04
	23.4	2.27	0.09

[a] 50 wt % PMDA–ODA + 50 wt % PMDA–PDA.
[b] 50 wt % BPDA–PDA + 50 wt % PMDA–PDA.

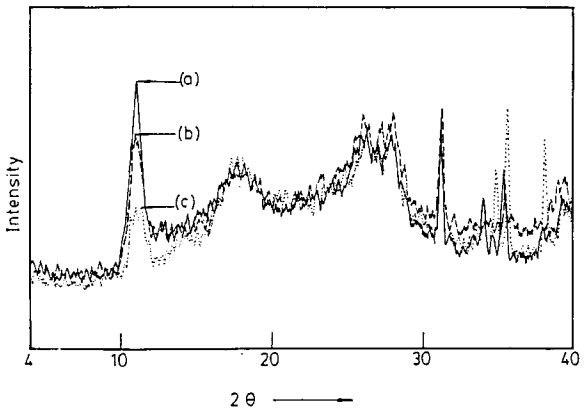

Figure 16 The in-plane X-ray diffraction patterns of the films of BPDA–PDA with various thicknesses: (a) 10.3 μm; (b) 17.2 μm; (c) 37.5 μm.

This work has been supported by the National Science Council, Taiwan, R.O.C., through projects NSC78-0405-E007-25 and NSC80-0405-E007-13.

REFERENCES

1. Y. Misawa, N. Monma, S. Numata, and N. Kinjo, *IEEE Trans. Electron Devices,* **ED-34,** 621 (1987).
2. R. J. Jenson, in *IEEE Electronic Components Conference,* 1984, p. 73.
3. F. K. Moghadam, *Solid State Technol.,* **27,** 149 (1984).
4. S. D. Senturia, in *Proceedings of the 2nd International Conference on Polyimides,* 1985, p. 107.
5. D. R. Day, in *Proceedings of the 1st International Conference on Polyimides,* 1982, p. 767.
6. T. Tchangai, Y. Segui, and K. Doukkali, *J. Appl. Polym. Sci.,* **38,** 305 (1989).
7. J. C. Wood, *Corrosion-NACE,* **34,** 70 (1978).
8. E. Sacher, *IEEE Trans. Electr. Insul.,* **EI-14,** 85 (1979).
9. G. Elsner, *J. Appl. Polym. Sci.,* **34,** 815 (1987).
10. S. T. Sackinger and R. J. Farris, *Polym. Mater. Sci. Eng.,* **57,** 356 (1987).
11. S. Numata, K. Fujisaki, and N. Kinjo, *Polymer,* **28,** 2282 (1987).
12. D. D. Denton, D. R. Day, D. F. Friore, and S. D. Senturia, *J. Electr. Mater.,* **14**(2), 119 (1985).
13. E. Sacher and J. R. Susko, *J. Appl. Polym. Sci.,* **23,** 2355 (1979).
14. E. Sacher and J. R. Susko, *J. Appl. Polym. Sci.,* **26,** 679 (1981).
15. D. K. Yang, W. J. Koros, H. B. Hopfenberg, and V. T. Stannett, *J. Appl. Polym. Sci.,* **30,** 1035 (1985).
16. D. K. Yang, W. J. Koros, H. B. Hopfenberg, and V. T. Stannett, *J. Appl. Polym. Sci.,* **31,** 1619 (1986).
17. B. D. Dean, *J. Appl. Polym. Sci.,* **33,** 2253 (1987).
18. S. A. Jinekhe and J. W. Lin, *Thin Solid Films,* **105,** 331 (1983).

19. B. S. Berry and W. C. Pritchet, *IBM J. Res. Dev.*, **28**(6), 662 (1984).
20. J. H. Jou, L. Hsu, P. T. Huang, W. P. Shen, and R. Huang, to appear.
21. C. E. Sroog, *J. Polym. Sci. Macromol. Rev.*, **11**, 161 (1976).
22. I. K. Varma, R. N. Geol, and D. S. Varma, *J. Polym. Sci. Polym. Chem. Ed.*, **17**, 5703 (1979).
23. J. Galiani, *Chem. Abstr.*, **91**, 159171g (1979).
24. J. H. Jou and P. T. Huang, in *Proceedings of the Annual Conference of the 13th ROC Polymer Symposium*, 1990, p. 481.
25. C. Goldsmith, P. Geldermans, F. Bedetti, and G. A. Walker, *J. Vac. Sci. Technol.*, **A1**, 407 (1983).
26. S. T. Chen, C. H. Yang, F. Faupel, and P. S. Ho, *J. Appl. Phys.*, **64**(12), 668 (1988).
27. J. Crank, *The Mathematics of Diffusion*, Oxford, Clarendon Press (1956).
28. J. H. Jou and P. T. Huang, *Polym. J.*, **22**, 909 (1990).
29. J. H. Jou, J. Hwang, and D. C. Hofer, *IBM-RJ* 5984 (59446), (1987).
30. S. T. Chen, C. H. Yang, H. M. Tong, and P. S. Ho, *MRS Symp. Proc.*, **79**, 351 (1987).
31. J. H. Jou and P. T. Hwang, in *Proceedings of the Annual Conference of the Chinese Society for Material Science*, 1030 (1990).
32. E. Gattiglia and T. P. Russell, *J. Polym. Sci. Polym. Phys. Ed.*, **27**, 2131 (1989).

Received August 31, 1990
Accepted December 3, 1990